

Influence of Rotations on the Critical State of Soil Mechanics

W. F. Oquendo^{1,3}, J. D. Muñoz^{1,3} and A. Lizcano^{2,3}

¹Simulation of Physical Systems Group, Department of Physics

Universidad Nacional de Colombia, Carrera 30 No. 45-03, Ed. 404, Of. 348, Bogota DC, Colombia

²Department of Civil and Environmental Engineering

Universidad de los Andes, Carrera 1 No. 18A-10, Bogota DC, Colombia

³CEIBA Complex Systems Research Center

CEiBA-Complejidad, Carrera 1 No. 18A-10, Bogota DC, Colombia

October 29, 2018

Abstract

The ability of grains to rotate can play a crucial role on the collective behavior of granular media. It has been observed in computer simulations that imposing a torque at the contacts modifies the force chains, making support chains less important. In this work we investigate the effect of a gradual hindering of the grains rotations on the so-called critical state of soil mechanics. The critical state is an asymptotic state independent of the initial solid fraction where deformations occur at a constant shear strength and compactness. We quantify the difficulty to rotate by a friction coefficient at the level of particles, acting like a threshold. We explore the effect of this particle-level friction coefficient on the critical state by means of molecular dynamics simulations of a simple shear test on a poly-disperse sphere packing. We found that the larger the difficulty to rotate, the larger the final shear strength of the sample. Other micro-mechanical variables, like the structural anisotropy and the distribution of forces, are also influenced by the threshold. These results reveal the key role of rotations on the critical behavior of soils and suggest the inclusion of rotational variables into their constitutive equations.

1 Introduction

Granular media is the second most used material by mankind, only after water [1, 2]. The annual production reaches almost 10 billions metric-ton/year. The industrial processing of these raw materials consumes nearly 10% of the total electric energy on Earth. Therefore, any optimization on the processing and any improve on the knowledge of GM will have a direct impact both on economy and welfare. Despite its ubiquitous nature, granular materials are far from being fully understood, mainly because of the numerous and different behaviors that can be generated collectively from the interactions of the particular grains. Granular media can behave as a liquid, solid or gas, and its particular behavior depends on the way the system is stimulated.

Soils represent a particular and important example of granular materials. They are the main subject of study for civil engineers dealing with settlements of buildings, earth pressure against retaining walls, stability of slopes and embankments, etc. Despite the rich complexity found in soils, like ratcheting and creep, there is a particular state that is independent of soil consolidation history, initial density and sample preparation: the critical state [3, 4, 5, 6, 7, 8]. In this steady state the deformation occurs at a constant average volume, void ratio, and effective stresses. The critical state has been characterized and stud-

ied from long time; however, its microscopic origins remain elusive.

The critical state is a fundamental concept in soil mechanics. It is linked with the so-called critical state constitutive models and failure criteria. Since the seminal work of Casagrande in 1936 [3], it has been found in sands and other types of granular media [3, 4, 5, 6, 9, 10, 11]. It is possible to reach the critical state through shearing, bi-axial or tri-axial tests. It is independent of the initial density, sample preparation or even shear rate, provided one is working in the quasi-static approximation.

The values of the macroscopic variables characterizing the critical state depend both on external and internal variables. External control variables are the confining pressure and the shear velocity; internal variables are the grains' size distribution and shape, the grain-to-grain friction coefficients, etc. It has been observed that the shape of the particles and its rotational freedom affect the final steady values [4, 5, 12]. In contrast with more complex shapes, spheres (or discs) favor rotations, because there is no geometric interlocking among them. If rotations are suppressed for spheres in some way, it is expected that the effective shear strength will increase. Suiker and Flerk [5] showed by three-dimensional computer simulations with spheres that a complete hindering of rotations modifies the critical shear strength. Similarly, A. A. Peña, R. García-Rojo and H. J. Herrmann [4, 9] studied the effect of particle shape on the critical state by using two particle kinds in 2D: almost isotropic and elongated. They found that both the void ratio and the coordination number at the critical state are different (among other variables) for isotropic and elongated particles. Nevertheless, no systematic study has been done regarding the role of rotations as a continuous parameter, for instance, by hindering gradually the rotations.

The main goal of the present work is to further explore the effect of restricting the rotation of the spheres on the macroscopic variables characterizing the critical state. This restriction is set by imposing a rotation threshold for each grain. The threshold is just the sum of the modulus of the normal forces on the grain times a rotational coefficient, which is the same for all grains. This procedure allows us

to mimic the effect of geometric interlocking, but increasing the hindering to rotate in a continuous way. In other words, we are simulating the effect of complex shapes by adding a rotation restriction on rounded grains. The effective shear strength, the mean coordination number, the effective stresses, and the force and torque distributions, will be investigated as a function of this rotational threshold. The study will be performed through molecular dynamics simulations of a bi-dimensional and periodic poly-disperse system under simple shear. Section 2 introduces the critical state and the computational setup. Section 3 describes the discrete-element model, that is the interactions among particles and the integration method for the equations of movement. Section 4 shows the main results and, finally, section 5 states the main conclusions from the work.

2 The Critical State

The critical state is defined in soil mechanics as the steady state where deformations occurs at constant average void ratio and effective stresses [13, 14] (Fig. 1).

The definition of the critical state can be expressed mathematically as

$$\frac{\partial \langle e \rangle}{\partial t} = \frac{\partial \langle p \rangle}{\partial t} = \frac{\partial \langle q \rangle}{\partial t} = 0 \quad , \quad (1)$$

where $\langle e \rangle$ is the average void ratio $e=V_V/V_S$ (i.e. the ratio between voids volume V_V and solids volume V_S), $\langle p \rangle$ is the average isotropic pressure, $\langle q \rangle$ is the average deviatoric pressure and ϵ_q is the deviatoric strain. In 2D, the mean pressure p is computed as $p=(\sigma_1 + \sigma_3)/2$, and the deviatoric stress as $q=(\sigma_1 - \sigma_3)/2$, where σ_1 (σ_3) is the principal value of the stress tensor on the axial (tangential) direction.

The inertia number I allows to quantify the degree of quasi-staticity of a given test [15, 16, 17, 18], and is defined as

$$I = \langle d \rangle \dot{\gamma} \sqrt{\frac{\rho}{\sigma_{wall}}} \quad , \quad (2)$$

where $\dot{\gamma}$ is the shear rate, $\langle d \rangle$ is the mean diameter, ρ is the density of the solid grains and σ_{wall} is the

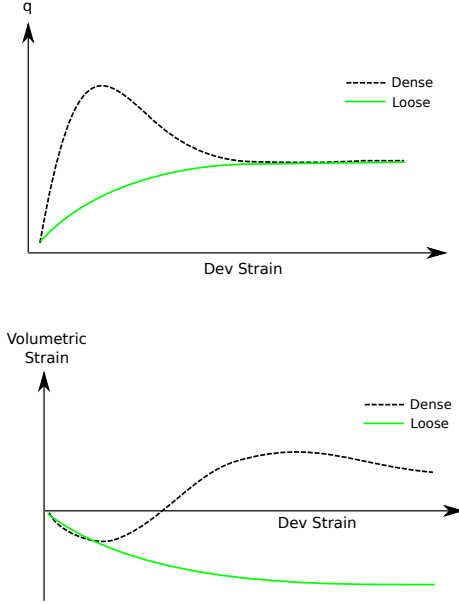


Figure 1: (Color online) (**Top**) Sketch of the typical responses for q , and (**Bottom**) of the volumetric strain, as functions of the deviatoric strain.

confining pressure. In a quasi-static test, $I \ll 1$. In this work, $I \simeq 10^{-3}$.

3 Discrete Element Method

We employed the *Discrete Element Method* (DEM), also known as Soft Particle method or Molecular Dynamics, to simulate the direct shear tests on two-dimensional poly-disperse samples of spheres. Since the movements are 2D, both the translational and rotational degrees of freedom are integrated with the Velocity Verlet method [19, 20, 21, 22].

The normal force between two grains (see Figure 2) is just the Hertz elastic law together with a damping term. It is given by

$$\vec{f}_n = \vec{f}_n^{el} + \vec{f}_n^{da} = k_{ij} \sqrt{R_{ij}} h_{ij}^{3/2} \hat{n}_{ij} - \gamma m_{ij} (\vec{v}_{ij} \circ \hat{n}_{ij}) \hat{n}_{ij} \quad (3)$$

where k_{ij} is the effective spring hardness, R_{ij} is the reduced radius, $h_{ij} = R_i + R_j - |\vec{r}_i - \vec{r}_j|$ is the mutual penetration, γ is the damping constant in normal di-

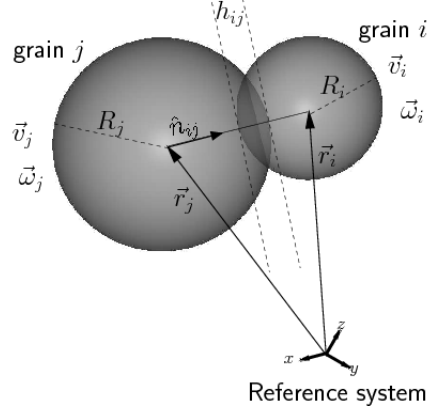


Figure 2: Relevant variables for the interaction among two spherical grains.

rection, m_{ij} is the reduced mass, $\vec{v}_{ij} = \vec{v}_i - \vec{v}_j$ is the relative velocity, and

$$\hat{n}_{ij} = \frac{\vec{r}_i - \vec{r}_j}{|\vec{r}_i - \vec{r}_j|} \quad (4)$$

For the tangential force we use the generalized Cundall-Strack model proposed by Luding [23], with a small correction for the tangential damping force. The algorithm is analogous for both sliding and rolling friction, and it reads as follows: As soon as a new contact appears (disappears) between two particles, a *virtual* spring is created (destroyed) for each of the friction processes aforementioned. This spring stores the relative tangential displacement. Let us denote the elongation of this tangential spring at time t by $\vec{\xi}$. The spring is always kept on the tangential direction by means of the transformation

$$\vec{\xi} = \vec{\xi} - (\hat{n}_{ij} \circ \vec{\xi}) \hat{n}_{ij} = \hat{n}_{ij} \times \vec{\xi} \times \hat{n}_{ij} \quad (5)$$

By using the current tangential spring elongation, a temporary tangential friction force \vec{f}_t^0 is computed as

$$\vec{f}_t^0 = -k_t R_{ij} \vec{\xi} - m_{ij} \gamma_t \vec{v}_t, \quad (6)$$

where k_t is a tangential stiffness, and γ_t is the tangential damping constant, which is introduced to improve the stability of the method [23]. Static friction

is present whenever $|\vec{f}_t^0| \leq \mu_s |\vec{f}_n|$; otherwise we are on the kinetic friction regime. In the static regime $\vec{f}_t = \vec{f}_t^0$, and the spring is updated as $\vec{\xi} = \vec{\xi} + \vec{v}_t \delta t$. In the kinetic regime, the tangential force is given by $\vec{f}_t = \mu_d |\vec{f}_n| \hat{t}_{ij}$, where μ_d is the kinetic friction coefficient (typically $\mu_d = 0.8\mu_s$), and the tangential unit vector \hat{t}_{ij} is defined dynamically as $\hat{t}_{ij} = \vec{f}_t^0 / |\vec{f}_t^0|$. The spring is updated as $\vec{\xi} = \frac{-1}{k_t} (\vec{f}_t + m_{ij} \gamma_t \vec{v}_t)$. The friction torque can be computed as

$$\tau = \vec{l}_i \times \vec{f}_t, \quad (7)$$

where \vec{l}_i is the branch vector from the center of the particle to the contact point. In total, four parameters are required for each tangential interaction: $k_t, \gamma_t, \mu_s, \mu_d$; but, in practice only μ_s is needed, since the other parameters are chosen relatively to the normal force parameters and μ_s itself.

A main goal of the simulation is to compute the macroscopic stress tensor $\sigma_{\alpha\beta}$. It is given by [24, 25]

$$\sigma_{\alpha\beta} = \frac{1}{V} \sum_{c \in V} f_\alpha^c l_\beta^c, \quad (8)$$

where V is the representative volume where the average is done, f_α is α -component of the force, l_β is the β -component of the branch vector (the vector joining the center of the particle to the point of contact) and the sum extends over all the contacts c among all particles inside the representative volume element. The structural anisotropy and mean coordination number are extracted from the fabric tensor, defined as

$$F_{\alpha\beta} = \frac{1}{N_c} \sum_{c \in V} n_\alpha^c n_\beta^c, \quad (9)$$

where \vec{n} is the normal vector joining the centers of two contacting particles, and the sum extends over the contacts c . The structural anisotropy is $a = 2(F_2 - F_1)$, where F_i is the i -th eigenvalue of the fabric tensor.

Finally, we define a rotational threshold coefficient μ_c to simulate the rotation resistance of complex shapes as follows: If the total torque $|\vec{T}_i|$ on the particle i is less than $\mu_c R_i \sum |\vec{F}_{n,i}|$, where $\sum |\vec{F}_{n,i}|$ is the sum of the normal forces on particle i , then the total

torque and the angular velocity are set to zero; otherwise they keep their current values. By this way it is possible to gradually hinder the rotation of the grains by changing the parameter μ_c . Since the sum of normal forces magnitudes depends on the number in contacts, this mechanism could reflect the interlocking of more general shapes, if rotation resistance is associated with geometric interlocking.

4 Results and Discussions

We have performed 2D simulations of periodic simple shear tests on a poly-disperse sample of 1024 discs. The radius of each particle is computed as [20]

$$R = \frac{R_{\min} R_{\max}}{R_{\max} - z(R_{\max} - R_{\min})}, \quad (10)$$

where $z \in [0, 1]$ is a random number. This particular form is uniform in *mass* (no size dominates the mass of the system), and generates more small particles than larger ones, as observed in natural soils. In contrast, the typical procedure of choosing the *radius* uniformly as

$$R = R_{\min} + z(R_{\max} - R_{\min}), \quad (11)$$

will generate almost the same number of small and large particles and concentrate the mass of system on the larger ones. In the present simulations, the ratio $R_{\max} : R_{\min} = 4 : 1$. The inter-particle static friction is 0.4. The rolling friction is 0.1. The full sample has been sheared (Figure 3), assuring that no localization band has appeared. In the following, numerical quantities like 1.23(4) should be interpreted as $1.23(4) = 1.23 \pm 0.04$, i.e. the error is in the last digit, where error bars correspond to three times the standard deviation. We checked that $\mu_c \simeq 2$ hinders the rotations almost completely, therefore there is no need to use larger values for this parameter.

4.1 Macroscopic internal friction

The ratio q/p as a function of the shear deformation ϵ_q is shown in Figure 4. First, the ratio grows almost linearly, until it gets the steady state, where it keeps

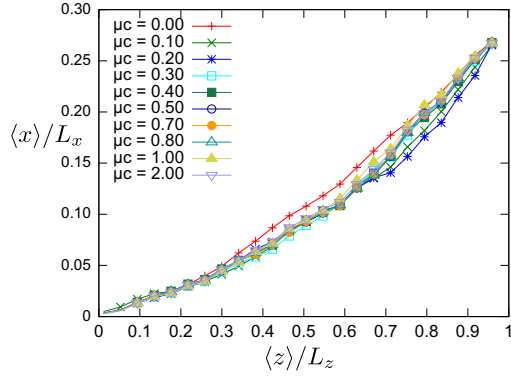


Figure 3: (Color online) Mean normalized horizontal translation as a function of the normalized height, for several values of the friction threshold μ_c . L_x and L_z are the horizontal and vertical size of the sample, respectively.

approximately the same mean value. The slope at the growing part represents a transient sample hardness. This hardness increases with the rotational threshold μ_c .

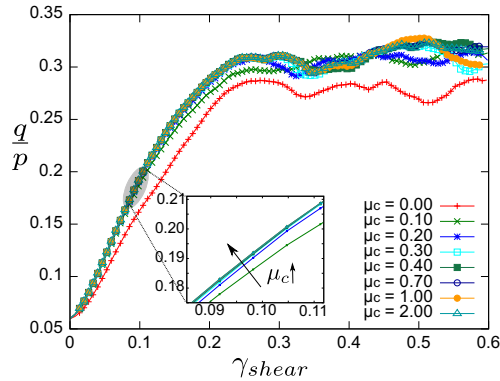


Figure 4: (Color online) q/p as a function of the shear deformation $\gamma_{shear} = \Delta x / L_z$, where Δx is the horizontal translation of the top wall, for several values of the threshold. The inset shows a zoom of the approximately linear growing regime.

As we stated before, the threshold μ_c represents a difficult for the particles to rotate, analogous to the

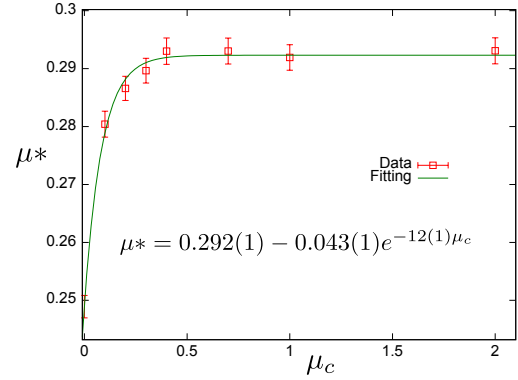


Figure 5: (Color online) Internal friction μ^* for several values of the threshold.

geometrical interlocking occurring in more complex-shaped bodies. It is well known [12] that irregular bodies has a large macroscopic internal friction angle $\mu^* = \tau / \sigma_{conf}$, where τ is the shear stress and σ_{conf} is the confining pressure, because of geometric interlocking. The shear strength μ^* of the sample increases with increasing μ_c (Figure 5). This support the interpretation of μ_c as quantifying the geometric interlocking of more complex shapes. The internal macroscopic friction μ^* grows like a saturated exponential with the form $\mu^* = 0.292(1) - 0.043(1)e^{-12(1)\mu_c}$. If μ_s increases, the final value of μ^* (equal to 0.292(1) in this case) also increases. Therefore, by tuning of μ_s and the threshold μ_c , it is possible to model samples of spheres with very high values of μ^* .

4.2 Distributions of Forces and Torques

The normalized distributions of forces and torques are presented in Figures 6 and 7 for several values of the rotational coefficient μ_c . Unexpectedly, it barely affects the general shape of the distribution of forces and torques in the sample.

It has been shown that normal forces, tangential forces and even the torques distribute as a power law for ranges smaller than the mean and as an exponen-

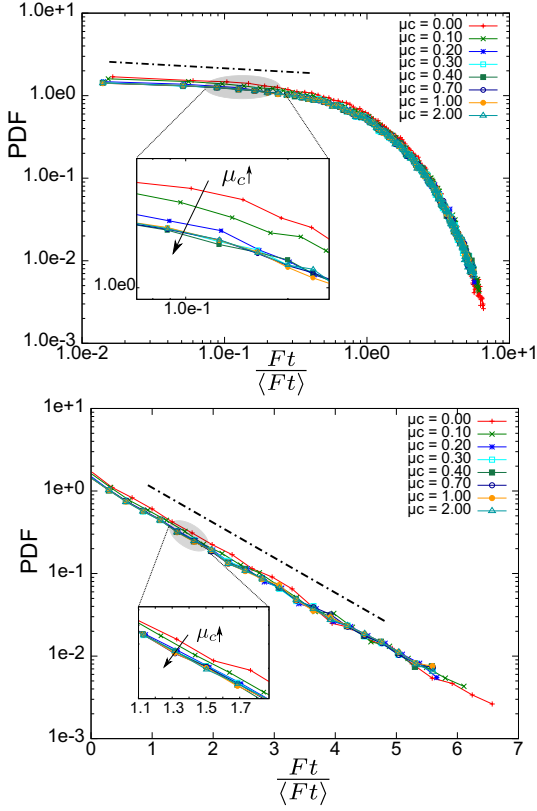


Figure 6: (Color online) Distribution of tangential forces at each contact, for several thresholds. Insets: Zoom on given ranges. (Top) Log-log, (Bottom) Linear-Log

tial for values larger than the mean [15, 26],

$$P(f) \propto \begin{cases} \left(\frac{f}{\langle f \rangle}\right)^\alpha, & f < \langle f \rangle, \\ e^{\beta[1-f/\langle f \rangle]}, & f > \langle f \rangle. \end{cases} \quad (12)$$

For all the values of μ_c , the exponents α and β are almost the same, $\alpha = -0.16(1)$, while for larger forces, $\beta = 0.93(2)$. Therefore, the forces' and torques' magnitudes distributions are barely affected by the threshold, although the relative importance of each particular distribution is slightly different.

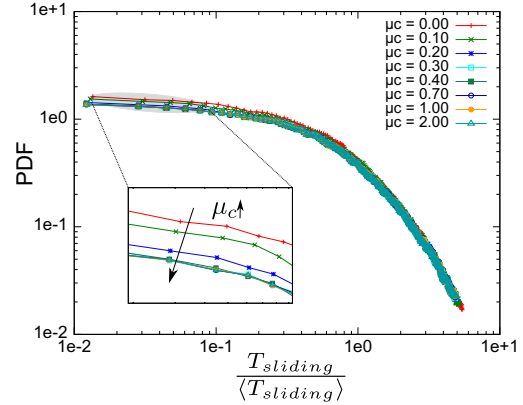


Figure 7: (Color online) Sliding torque distributions for several thresholds. Inset: zoom in the range of small forces

4.3 Mean Coordination number and structural anisotropy

The mean coordination number, on one hand, is almost constant for all the values of μ_c , with a value of $\langle z \rangle = 4.1(2)$. On the other hand, the structural anisotropy starts with a small value and decays rapidly to almost a constant value for large thresholds (Fig. 8).

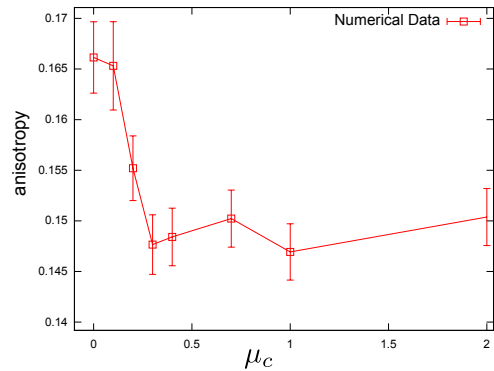


Figure 8: (Color online) Structural anisotropy as a function of the thresholds.

Although the mean contact number is practically the same for all thresholds, we found that the larger

the threshold the smaller the structural anisotropy. This result agrees with [12], where discs' and pentagons' samples were compared in biaxial tests and it was found that discs' samples have higher structural signed anisotropies and smaller strengths, because of smaller force anisotropy. If the threshold μ_c can be associated with shape, then larger values of μ_c should reflect more irregular shape, higher shear strength and smaller structural anisotropy, as found. The higher shear strength with smaller structural anisotropy can be explained by means of the forces' anisotropies, that reflects how the forces magnitudes are distributed along the contact network. Future works could check that increasing μ_c enhances the force anisotropies and thus the shear strength. Since the structural anisotropy decreases rapidly to a constant value, the parameter μ_c is shown to captures some but not all the effects of irregular shapes. For increasing values of μ_c , the connectivity of the contact network is kept constant in average, while the quantities that are carried over this network are changing, since $\langle z \rangle$ is almost constant while the structural anisotropy decreases for increasing μ_c .

5 Conclusions

In this work we studied the effect of a gradual hindering of the rotations on the critical state of a two-dimensional dry soil of poly-disperse spheres with size span 4:1. For this purpose, we have simulated a simple shear test for several values of a rotational threshold friction coefficient μ_c , acting as follows: the rotation of a sphere is allowed only if the magnitude of the total torque on the sphere is larger than the sum of the magnitudes of the normal forces at all contacts times the threshold μ_c . So, if $\mu_c = 0$ all torques (and its respective effect on rotations) are allowed, while if $\mu_c \rightarrow \infty$, no rotation occurs. Actually, we found that values of $\mu_c \simeq 2$ are enough to hinder almost completely all rotations.

In order to characterize the effect of μ_c on the macroscopic response of the system, five quantities were tracked: the stress ratio q/p , the total internal friction μ^* , the distribution of forces and torques, the mean correlation number $\langle z \rangle$, and the structural

anisotropy of the fabric tensor. We found that the final stress ratio q/p is slightly increased for larger values of μ_c ; a consistent increment of the sample hardness before the critical state is reached can be easily observed. The normalized distribution of forces' and torques' magnitudes are barely affected in terms of its characteristic exponents, although its relative importance seems to decrease for higher values of μ_c . The mean correlation number is barely affected by the rotational threshold μ_c , which means that the connectivity of the contact network is not changed. In contrast, the macroscopic friction coefficient μ^* does increase with μ_c , like a saturated exponential, while the structural anisotropy decreases. This last result agrees with previous hindering strategies at the level of contact (instead of at the level of particles as here) [12]. This results enhances the interpretation of μ_c as characterizing the effect of complex shapes and its natural geometric interlocking. Further works could check the evolution of the force anisotropies in order to explain the increasing shear strength with decreasing structural anisotropies. We expect the force anisotropies to increase with μ_c . The threshold μ_c captures some but not all the features of more complex shapes.

Different values of the static friction coefficient between grains produce different values for the global internal friction coefficient μ^* , and the value of the later can be further increased by means of the threshold μ_c . This relationship can be exploited to simulate materials composed of spheres and with very high strengths, but further calibration with models including irregular shapes is needed.

This work is a contribution to a better understanding of the critical state and the role of the rotational degrees of freedom. The exact dependence for different macroscopic parameters, for different macroscopic conditions, the role of forces anisotropies, and its quantitative comparison with more complex shape materials are topics of future work.

6 Acknowledgments

We thank the CEiBA complex systems research center for financial support, and Nicolás Estrada and

Mauricio Botton for helpful discussions.

References

- [1] P. G. de Gennes, Granular matter: a tentative view, *Reviews of Modern Physics* 71 (2) (1999) 374–381, centenary 1999.
- [2] J. Duran, *Sands, Powders, and Grains: An Introduction to the Physics of Granular Materials (Partially Ordered Systems)*, 1st Edition, Springer, 1999, p.-G.de Gennes (Foreword).
- [3] A. Casagrande, Characteristics of cohesionless soils affecting the stability of slopes and earth fills, *J. Boston Soc. Civil Engineers* 23 (1) (1936) 13–32.
- [4] A. A. Peña, Influence of particle shape on the global mechanical response of granular packings: Micromechanical investigation of the critical state in soil mechanics, Ph.D. thesis, Institut für Geotechnik der Universität Stuttgart (2008).
- [5] A. S. J. Suiker, N. A. Fleck, Frictional collapse of granular assemblies, *Journal of Applied Mechanics* 71.
- [6] W. Wu, E. Bauer, D. Kolymbas, Hypoplastic constitutive model with critical state for granular materials, *Mechanics of Materials* 23 (1996) 45–69.
- [7] H. Hinrichsen, D. E. Wolf (Eds.), *The physics of granular media*, Vch Verlagsgesellschaft Mbh, 2004.
- [8] F. Radjai, S. Roux, Contact Dynamics Study of 2D Granular Media: Critical States and Relevant Internal Variables, Ch. 7, Vol. 1 of Hinrichsen and Wolf [7].
- [9] A. A. Peña, R. García-Rojo, H. J. Herrmann, Influence of particle shape on sheared dense granular media, *Granular Matter* 9 (2007) 279–291.
- [10] H. Hinrichsen, D. E. Wolf (Eds.), *Contact Dynamics Study of 2D Granular Media: Critical States and Relevant Internal Variables*, Wiley - VCH, 2004.
- [11] S. Antony, W. Hoyle, Y. Ding, *Granular materials: fundamentals and applications*, Royal Society of Chemistry, 2004.
- [12] E. Azéma, F. Radjai, R. Peyroux, G. Saussine, Force transmission in a packing of pentagonal particles, *Phys. Rev. E* 76 (1) (2007) 011301. doi:10.1103/PhysRevE.76.011301.
- [13] D. Wood, *Soil Behaviour and Critical State Soil Mechanics*, Cambridge University Press, 1990.
- [14] J. Atkinson, *An Introduction to the Mechanics of Soils and Foundations Through Critical State Soil Mechanics*, Mac Graw Hill, 1993.
- [15] N. Estrada, A. Taboada, F. Radjai, Shear strength and force transmission in granular media with rolling resistance, *Phys. Rev. E* 78 (021301).
- [16] G. MiDi, On dense granular flows, *The European Physical Journal E: Soft Matter and Biological Physics* 14 (4) (2004) 341–365.
- [17] F. Da Cruz, S. Emam, M. Prochnow, J. Roux, F. Chevoir, Rheophysics of dense granular materials: Discrete simulation of plane shear flows, *Physical Review E* 72 (2) (2005) 21309.
- [18] I. Agnolin, J.-N. Roux, Internal states of model isotropic granular packings. iii. elastic properties, *Physical Review E (Statistical, Nonlinear, and Soft Matter Physics)* 76 (6) (2007) 061304. doi:10.1103/PhysRevE.76.061304. URL <http://link.aps.org/abstract/PRE/v76/e061304>
- [19] D. C. Rapaport, *The Art of Molecular Dynamics Simulation*, second edition Edition, Cambridge University Press, 2004, molecular Dynamics.
- [20] T. Pöschel, T. Schwager, *Computational Granular Dynamics*, Springer, 2004.

- [21] W. C. Swope, H. C. Andersen, P. H. Berens, K. R. Wilson, A computer simulation method for the calculation of equilibrium constants for the formation of physical cluster of molecules: applications to small water clusters, *J. Chem. Phys* 76 (1982) 637–49.
- [22] W. F. Oquendo, J. D. Muñoz, A. Lizcano, Oedometric test, bauer’s law and the micro-macro connection for a dry sand, *Computer Physics Communications* 180 (4) (2009) 616–620, iSSN 0010-4655, DOI: 10.1016/j.cpc.2009.01.002.
- [23] S. Luding, Cohesive, frictional powders: contact models for tension, *Granular Matter* 10 (4) (2008) 235–246.
- [24] J. J. Moreau, Friction, Arching, Contact Dynamics, World scientific Singapore, 1997, pp. 233–247.
- [25] L. Staron, F. Radjai, J. Vilotte, Multi-scale analysis of the stress state in a granular slope in transition to failure, *The European Physical Journal E: Soft Matter and Biological Physics* 18 (3) (2005) 311–320.
- [26] F. Radjai, M. Jean, J. Moreau, S. Roux, Force distributions in dense two-dimensional granular systems, *Physical Review Letters* 77 (2) (1996) 274–277.